Available online at www.sciencedirect.com
SCIENCE DIRECT®
Remote Sensing of Environment 102 (2006) 328–343
Remote Sensing of Environment
www.elsevier.com/locate/rse

Using bi-directional soil spectral reflectance to model soil surface changes induced by rainfall and wind-tunnel abrasion

Adrian Chappell [a,*], Ted M. Zobeck [b], Gillian Brunner [a]

[a] Centre for Environmental Systems Research, University of Salford, Manchester, M5 4WT, UK
[b] USDA, Agricultural Research Service, Cropping Systems Research Laboratory, Lubbock, TX 79415, USA

Received 10 January 2006; received in revised form 21 February 2006; accepted 25 February 2006

Abstract

To improve wind erosion model calculations across several spatial and temporal scales simultaneously, there is a requirement for a non-invasive approach that can be used rapidly to assess changes in the compositional and structural nature of a soil surface in time and space. Remote sensing allows consideration of the processes controlling erodibility on the same spatial continuum to avoid time-consuming and expensive fieldwork. Multi-angular spectral reflectance appears to provide a holistic framework for the measurement and calculation of soil surface characteristics remotely using ground-based radiometers and current and future generations of angular sensors on airborne and satellite platforms. To investigate the utility of this framework, a ground-based study was performed using three soils susceptible to wind erosion that were modified using rainfall simulation and wind tunnel abrasion experiments. Measurements of those changes were made and recorded using digital images. Multi-angular spectral measurements of reflectance were also made and inverted against a bi-directional soil spectral reflectance model. Comparison of the measurements and calculations showed good agreement with small errors in accuracy. Optimised values of the model parameters produced the single scattering albedo and a description of the reflectance scattering behaviour of the soil surfaces that included an estimate of roughness. The model parameters removed the effect of illumination and viewing geometry on the spectral reflectance. The combination of single-scattering albedo spectra and model parameters for each treatment provided information about the composition and structure of the soil surface changes. The main changes detected at the soil surface included the presence of a crust produced by rain-splash, the production of loose erodible material covering a rain crust and the selective erosion of the soil surface. Redundancy analysis showed that much of the variation in the values of the soil reflectance model parameters was explained by the scattering properties and the roughness parameter of the soil surfaces. Variation in the soil surface reflectance was not explained solely by soil type. Instead, low intensity rainfall combined with short and long duration abrasion explained a significant portion. These findings provide a source of considerable variation in experimental and operational spectral reflectance measurements that has perhaps hitherto been largely ignored. The results demonstrated the readily available information on the composition and structure of the soil surface without interfering with natural processes. The directional soil reflectance methodology appears to have potential for use in improving the understanding of erodibility and ultimately for identifying and quantifying soil erosion.

Keywords: Wind erosion; Soil erodibility; Wind tunnel; Rainfall simulator; Bi-directional soil spectral reflectance model; Canonical ordination; Redundancy analysis

1. Introduction

Wind erosion is an important problem that threatens 30 million ha of land in the United States. On cropland in the USA, about 28 million ha are eroded by wind at rates that exceed twice the tolerance level for sustainable production (USDA, 1989). Much of Australia is also affected by wind erosion and more than half of its area is in need of soil conservation treatment, and approximately one eighth is so badly damaged by agriculture that repair work is urgently needed (Beale & Fray, 1990). Cattle grazing in Queensland is very extensive but small annual rainfall and large stocking rates have removed natural vegetation cover and broken soil crusts, which protect the soil from wind erosion (McTainsh et al., 1998). From a land resource perspective and in terms of sustainable agriculture it is important to accurately determine wind erosion across several spatial scales to identify the controlling environmental processes. Thus, there is a growing

* Corresponding author. Tel.: +44 161 295 3653; fax: +44 161 295 5015.
E-mail address: a.chappell@salford.ac.uk (A. Chappell).

0034-4257/$ - see front matter
doi:10.1016/j.rse.2006.02.020

need for the estimation of source areas and the intensity of dust emission at several spatial scales that can realistically only be handled by wind erosion models (Shao & Leslie, 1997).

Recent developments in wind erosion models (e.g., Böhner et al., 2003; Fryrear et al., 1998; Shao & Leslie, 1997) and models of dust emission (e.g., Marticorena & Bergametti, 1995; Sokolik & Toon, 1996; Zender et al., 2003) have also highlighted the need for information on the spatial and temporal variation of composition, aggregation and roughness because these soil surface conditions control the surface susceptibility to wind erosion (erodibility) and hence the emission of dust (Zobeck, 1991b). Shao et al. (1996) suggested that the main limitation of wind erosion models is their inability to incorporate the evolution of surface soil conditions. The SOIL sub-model in the USDA-Agricultural Research Service, Wind Erosion Prediction System (WEPS) model was developed in recognition that the soil's aggregation and surface state can dramatically affect erodibility (Hagen et al., 1995). Thus, changes in soil and surface temporal properties are simulated daily by the model. Soil layer properties such as bulk density, aggregate size distribution and dry aggregate density are maintained on a daily basis. Surface properties such as random and oriented roughness, crust generation, coverage fraction, density, stability and thickness and loose erodible material on crusted surfaces are also taken into account (Wagner, 1995). Collection of these data, even in the USA, is often limited to individual agricultural fields or administrative regions because in situ measurements are labour-intensive and very time-consuming and experiments to understand the variation of erodibility over several spatial and temporal scales are prohibitively expensive. Arguably, these field-based approaches are even inadequate at the field scale where soil surface conditions vary considerably and evolve simultaneously in space and time. Shao et al. (1996) provided one of the first physically based wind erosion models to operate across spatial scales from the field to the continent (Australia). One of the main reasons for its success was its inclusion of remote sensing data. However, Shao and Leslie (1997) suggested that the Shao et al. (1996) model required more detailed estimation of erodibility, in particular the estimation of surface roughness elements, soil water content and surface crusting. They suggested that the dynamic effect of surface roughness elements is difficult to describe because surfaces are often composed of standing roughness elements, flat surface covers, tillage ridges and various levels of random roughness elements (Potter et al., 1990).

To improve wind erosion model calculations across several spatial and temporal scales simultaneously requires a non-invasive approach that can be used to rapidly assess changes in the compositional and structural nature of a soil surface in time and space. Furthermore, the approach is required to provide a holistic framework so that the factors controlling the processes of erodibility may be considered on the same continuum (Geeves et al., 2000). One approach to providing this information is to use remote sensing to measure soil surface reflectance frequently and at many locations across relatively large areas simultaneously. Measurements of the intrinsic optical properties of the soil surface produce wavelength-specific absorption of electromagnetic radiation, yielding diagnostic reflectance spectra for the properties under investigation. Observed spectral variations will provide information on the chemical composition of the soils involved, whilst directional variations will elucidate the structure of the materials under investigation. The main controls on soil surface reflectance variation; organic matter, soil water, mineralogy, particle size and surface roughness (Huete & Escadafal, 1991;

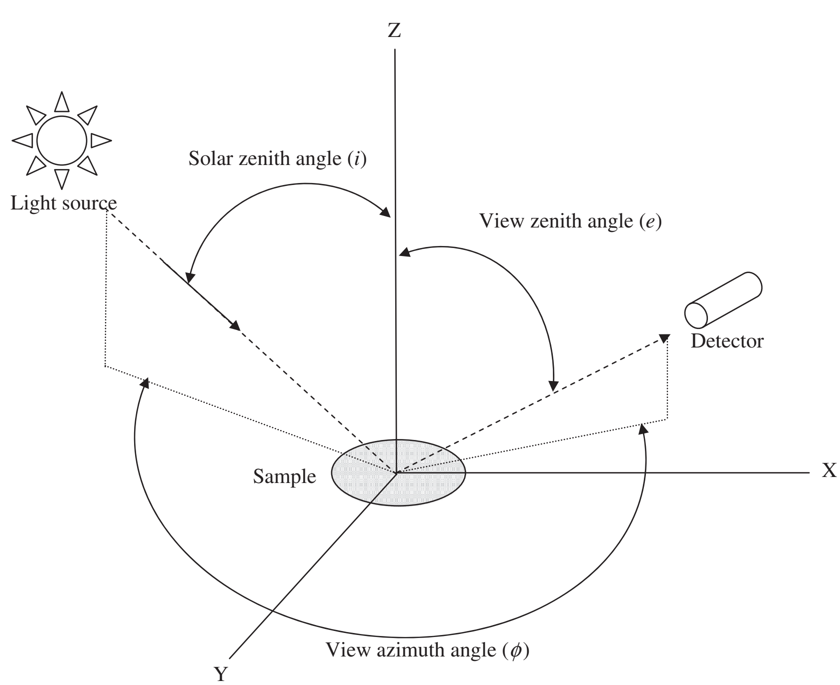

Fig. 1. Illumination and viewing angles used in the soil bi-directional spectral reflectance model of Jacquemoud et al. (1992).

Price, 1990) are also those that affect (either directly or indirectly) the soil surface erodibility by wind. Thus, there is a strong potential for developing a physical relationship between spectral reflectance and erodibility (e.g., Baumgardner et al., 1985; Latz et al., 1984; Seubert et al., 1979). Furthermore, non-wavelength specific or structural soil factors such as roughness can be deduced by examining the reflectance at all possible illumination and sensor view angles of a particular target as represented by the Bi-directional Reflectance Distribution Function (BRDF). Bi-directional soil spectral reflectance models (Hapke, 1963; Jacquemoud et al., 1992; Pinty et al., 1989) that can be readily inverted against multi-angular spectral reflectance measurements offer a potential framework to unify the investigation of soil surface erodibility by wind and perhaps quantify wind erosion. This framework also lends itself to multi-scale assessments across large areas using existing and forthcoming generations of angular sensors on airborne and satellite platforms. However, because of differences in resolution and scale between laboratory/field-based measurements and space-borne sensors there remains outstanding a considerable amount of research to understand the nature of the retrieved information.

The aim here is to examine under controlled conditions the extent to which a bi-directional soil spectral reflectance model (Jacquemoud et al., 1992) can retrieve information on the variability of soil surface conditions. The approach used here develops from earlier work (Chappell et al., 2005) that showed as much variation in the spectral reflectance of soil surface conditions within a soil type as there was between soil types. Therefore, samples of three soil types susceptible to wind erosion were prepared and modified, using wind tunnel and rainfall simulators, to recreate in the laboratory, soil surface conditions typical of the natural environment. This paper is an attempt to move towards the larger research goal to show how a remote sensing approach enables the concept of erodibility to be considered on a continuum in terms of its spatial and temporal variation and how a single framework (multi-angular spectral reflectance) can integrate the assessment of soil surface composition and structure.

2. Methods

2.1. Bi-directional reflectance model and parameters

Using the fundamental principles of radiative transfer theory, Hapke (1963, 1981) derived an analytical equation for the bi-directional reflectance function of a medium composed of dimensionless particles and applied it to planetary surfaces such as the moon. Pinty et al. (1989) extended that work to describe soil surfaces on Earth where individual particles have non-uniform angular distributions and Pinty and Verstraete (1991) included a more complex description of the 'hot spot'. Jacquemoud et al. (1992) provided a simplified formulation which required six parameters and attempted an explanation of both backward and forward scattering (the specular effect) of light by smooth soils as a consequence of the material of which it is composed. Thus, the model and its parameters are likely to be useful for characterising the soil surface and changes to it. It is used here and described below.

Hapke's model assumed that a plane surface at $z=0$ contained irregular and randomly orientated particles that are large compared with the wavelength. The bi-directional reflectance r of a surface illuminated with a solar zenith angle i, viewed from a zenith angle e (Fig. 1) and normalised with respect to the reflectance of a perfectly reflecting Lambertian surface under the same conditions of illumination and observation is given by:

$$r(i,e,\phi) = \frac{\omega}{4}\frac{1}{\cos i + \cos e} \times \{[1 + B(g)]P(g,g') + H(\cos i)H(\cos e) - 1\} \quad (1)$$

where,

$$\cos g = \cos i \cos e + \sin i \sin e \cos\phi,$$

$$\cos g' = \cos i \cos e - \sin i \sin e \cos\phi,$$

$$B(g) = \frac{1}{1 + (1/h)\tan(g/2)},$$

$$P(g,g') = 1 + b\cos g + c\frac{3\cos^2 g - 1}{2} + b'\cos g' + c'\frac{3\cos^2 g' - 1}{2}, \quad \text{and}$$

$$H(x) = \frac{1 + 2x}{1 + 2\sqrt{(1-\omega)}x}.$$

In Eq. (1), ϕ is the viewing azimuth relative to the Sun's azimuth, ω is the single scattering albedo (the ratio of the scattered energy to the total energy either scattered or absorbed by the particle), g is the phase angle between the incoming and outgoing light directions, g' is the angle between the specular and the outgoing light directions. The function $B(g)$ explains backscattering of light as a function of g and a roughness parameter h which is related to the grain size distribution, the porosity of the medium and gradient of compaction with depth (Hapke, 1963). In other words, as the surface becomes smooth, h increases. The type of scattering is related to the surface roughness and the nature of the particles. The phase function $P(g,g')$ describes the angular distribution of the light scattered by a terrestrial surface. The term $H(\cos i)H(\cos e) - 1$ approximates the contribution from multiple scattering following Pinty et al. (1989) and x is used to indicate the substitution of the cos i and cos e terms into the equation, respectively. Three different types of reflectances were demonstrated as part of the model derivation (Jacquemoud et al., 1992; p. 125): backscattering has values for parameters b and c that are larger than those for b' and c'; forward scattering has values for b' and c' that are larger than those of b and c, and mixed scattering has values for b and c that are similar to those for b' and c'.

Table 1
Geometries of measurement for directional spectral data

Source		Sensor
i	ϕ	e
53	0	0, −10, −20, −30, −40, −50, +10
53	180	0, +10, +20, +30, +40, +50, −10
53	270	0, +10, +20, +30, +40, +50, −10, −20, −30, −40, −50

The surface was illuminated with a lamp zenith angle i and azimuth angle ϕ, and viewed from a negative (−) or positive (+) zenith angle e.

2.2. Application and sensitivity of the model

Pinty et al. (1989) suggested that the key problem with the measurement of spectral reflectance data is its interpretation in terms of the physical quantities of interest for the observed surface. Furthermore, if the radiometric properties of a bare soil surface can be described by Eq. (1), the interpretation problem consists of finding the values of the six parameters such that the computed value of r best approximates the actual observations. Following Pinty et al. (1989) and Jacquemoud et al. (1992) a non-linear least squares fitting procedure was used to solve the inverse problem for the quantity δ^2:

$$\delta^2 = \sum_{k=1}^{n} [r_k - r(i_k, e_k, g_k)]^2, \tag{2}$$

where r_k is the measured bi-directional reflectance of the surface for the relative geometry of illumination and observation defined by i_k, e_k, g_k, n is the total number of observations and r is the calculated bi-directional reflectance. The problem then reduces to finding the optimal values of the parameters, which minimises δ^2 for a set of measurements. The performance of the optimisation is judged using the square root of mean squared difference (RMSE) $\sqrt{\delta^2/N_f}$, where N_f is the number of degrees of freedom, which is the number of independent data points minus the number of parameters estimated by the procedure. This inverse modelling problem was coded in Matlab using 'lsqnonlin'. The code implements either a Gauss–Newton or a Levenberg–Marquardt method depending on performance (Matlab, 2000) subject to fixed upper and lower bounds on the independent variables using function values alone. It requires an initial estimate for each of the parameters and it is important to establish the sensitivity of the retrieved values of the parameters to those initial estimates.

The sensitivity of the model parameters for bi-directional reflectance using this model inversion approach was investigated by Pinty et al. (1989) and followed by Jacquemoud et al. (1992). The first sensitivity experiment performed by Pinty et al. (1989) was repeated here (not shown) and demonstrated that the values of the retrieved model parameters and of the RMSE did not depend on the initial estimate. Pinty et al. (1989) also showed that the accuracy of the inversion procedure increased with finer resolution of sampling in the solar and viewing angles. The data used in the model inversion for this paper were obtained from a consistent sampling resolution to ensure repeatable retrieval of the model parameters (Table 1). The final sensitivity experiment performed by Pinty et al. (1989) is performed here to quantify the maximum amount of random noise in the data that could be tolerated before the retrieved parameters might become unacceptably different from their true values.

2.3. Directional spectral reflectance measurements

The Analytical Spectral Devices (ASD) spectroradiometer used here had a spectral range of 350–2500 nm and spectral sampling of 1.4 nm between 350 and 1050 nm and 2 nm between 1000 and 2500 nm. An 8° field of view was used and illumination was provided by a 1000 W Halogen lamp, which had a zenith angle of 53°. A goniometer allowed repeatable and consistent measurements of multi-angular reflectance of the soil surface and enabled several view zenith and azimuth angles (Table 1).

In the experiments conducted here, a calibrated Spectralon panel provided total irradiance information. Two Spectralon reflectance reference measurements were made immediately before and after the target measurements under the same conditions as the measurement. Conversion to spectral reflectance was conducted by dividing the reflectance spectra of the soil samples by the spectra of a white Spectralon reference panel. The soils were placed under the sensor at exactly the same location. The radiometer had a video camera strapped to it so that images of the soil surface were also captured at the same time as on-nadir reflectance to provide a visual record of changes to the soil surface composition and structure during the experiments.

2.4. Soil types and property measurements

Three fine soil types were used in the experiments and Table 2 provides some of their characteristics. The soil types chosen were susceptible to wind erosion on agricultural land that was close to where the experiments were conducted in the

Table 2
Some characteristics of the soils used in the experiments (modified from Chappell et al., 2005)

Soil type (label)	Soil munsell dry colour	Fe (%)	pH	Organic carbon (%)	Median particle size (μm)	Sand content (%)	Silt content (%)	Clay content (%)
Amarillo fine sand (FS)	7.5YR 5/6	0.26	7.53±0.034	0.34±0.008	176.2	89.1	4.0	6.9
Amarillo fine sandy loam (FSL)	7.5YR 4/4	0.53	7.99±0.005	0.83±0.091	88.3	63.4	18.2	18.4
Randall clay loam (CL)	7.5YR 5/2	0.55	7.07±0.005	1.09±0.010	43.4	44.9	22.7	32.4
Abrader sand (ABS)	10YR 7/2	–	–	–	728.9	100.0	4.0	6.9

–: missing data.

vicinity of the United Stated Department of Agriculture (USDA) Agricultural Research Service (ARS) in Lubbock, Texas. The soil types were also used to represent the variation in texture, an important factor controlling wind erosion. The first type (FS) was an Amarillo fine sand, which was a mixed, superactive, thermic Aridic Paleustalf. The second (FSL) was an Amarillo fine sandy loam. The third soil type (CL) was a Randall clay loam which was a smectitic, thermic Ustic Epiaquert. All of the soils were from the Ap horizon. An abrader was used in the wind tunnel experiments and the characteristics of this material are also shown in Table 2. Details of the soil measurement procedures are contained in an earlier paper (Chappell et al., 2005).

2.5. Soil treatment experiments

Straightforward experiments involving a rainfall simulator, drying ovens and a wind tunnel were used to induce changes in the surfaces of each soil type. The experiments were developed to include simulations of natural environmental processes that were known to alter the soil surface condition. Details of the experiments can be found elsewhere (Chappell et al., 2005). In preparation for the experiment each soil was passed through a 2 mm mesh and loaded into 2507 cm^2 sample trays (54.5 cm × 46 cm). The tray bases comprised wire mesh and muslin material to allow water drainage whilst minimising soil loss. The tray sides were adjustable and were standardised at a thickness of 6.5 cm during the loading process. A straightedge was used to smooth the surface and remove initial inconsistencies between soils and individual trays. The sides were lowered during the experiments to account for surface lowering during wind erosion. Directional reflectance measurements were taken before any experiments were conducted. After the soils were exposed to either low or high intensity rainfall simulation, they were placed in drying ovens. After drying in the oven, directional reflectance was measured once again and it was also measured after 1 min and 8 min of abrasion. Amongst other things, the earlier experiment (Chappell et al., 2005) found that variation in surface conditions for a soil type was a source of considerable variation in spectral reflectance that has been largely ignored. Thus, it is likely that variation in environmental treatments within a soil type is a simple and underestimated source of variation in the characterisation of soil surface erodibility and in the remote sensing of soil.

2.6. Canonical ordination (redundancy analysis) of soil spectral reflectance

Redundancy analysis (RDA) was used here to establish the relations between model parameter values, soil type and soil treatment. The technique was used by Chappell et al. (2005) with considerable success to simplify the relationship between spectral reflectance changes with treatment. As with that previous analysis, the program CANOCO (version 4.02; Ter Braak, 1988) was used for RDA. The model parameter values were not transformed. Samples were standardised and wavebands were centred and standardised. A focus on scaling of inter-sample distances was used to interpret the relationships among model parameter values from the ordination diagram. The model parameter values were divided (after extraction of their axes) by their standard deviations so that the ordination diagram displayed standardised reflectance data and correlations instead of covariances. A vector drawn from the origin of the ordination diagram to each model parameter represents the fit (correlation) with the ordination axis, i.e., vectors close to an axis are highly correlated with the information extracted by that axis. The treatment indicators were represented on the ordination diagram by plotting the centroids of their samples. Similarity between the model parameter vectors and those of the treatment centroids quantify the correlation between the two

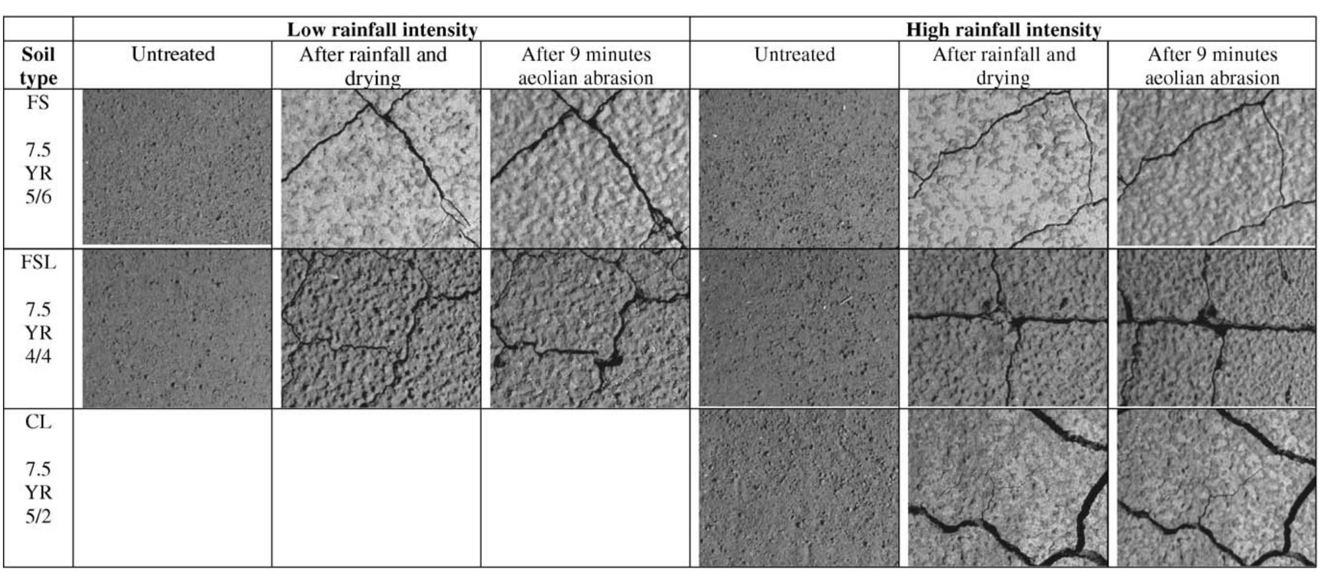

Fig. 2. Portions (ca. 300 mm × 200 mm) of nadir video images taken before treatment, after low and high rainfall intensity and drying treatment and after an accumulated 9 minute aeolian abrasion treatment for each soil type (see text for details). Modified from Chappell et al. (2005).

types of data. Vectors oriented in approximately the same direction indicate strong positive correlation, whilst those oriented in opposite directions imply strong negative correlation. Vectors orthogonal to one another were uncorrelated.

The most significant predictive variables were selected after the removal of redundant variables with large multicollinearity. A forward selection procedure which used a Monte Carlo permutation test at each selection step was used to test the statistical significance of the variance explained by each variable added to the model (Ter Braak, 1988).

3. Results

3.1. Soil characteristics and visual observations during treatments

Table 2 shows the characteristics of the soils. The median particle size represents the particle size distribution for each soil type. The FS soil is generally coarser, has more sand and the smallest silt and clay content than the other soil types. The CL soil is generally the finest material, has the least sand and the largest content of silt and clay. The FSL has intermediate amounts of the sand size fraction and notably similar proportions of clay and silt. The abrader material comprised washed sand and was much coarser than the soils.

The organic carbon content is smallest in soil FS, intermediate in soil FSL and the largest content is found in soil CL. The pH of those soils does not follow the same pattern. That of soil FSL is considerably larger than the other soil types. The pH of soil FS is the next largest, whilst that of soil CL has the smallest pH. Munsell colour designations are also listed for all soils in Table 2. All soils had a brown to strong brown colour with only slight differences in value or chroma. The CL soil had the lowest chroma, with a Munsell colour of 7.5YR 5/2. Soil FS had a slightly stronger brown colour with a higher chroma, 7.5YR 5/6. Soil FSL had the lowest value at 7.5YR 4/4. The abrader material was light gray, with a Munsell colour designation of 10YR 7/2.

The images taken before the treatments, after rainfall and drying and after abrasion are shown in greyscale in Fig. 2. The untreated soils appear similarly unconsolidated and the surface particles are aggregated. The rainfall treatment changed the brightness of soils, compared to the untreated condition. Regardless of the rainfall intensity, all soils were crusted, cracked and showed evidence of rain-splash erosion (induced roughness). The CL soil did not appear to exhibit a change in

Table 3
Sensitivity analysis showing the average of the optimised values for the parameters in the soil bi-directional reflectance model of Jacquemoud et al. (1992)

		Bi-directional reflectance model parameters							
	Added noise (S.D.)	ω	b	c	h	b'	c'	N	RMSE
A)									
True		0.500	0.150	−0.320	1.990	1.410	−0.450		
Initial (i)		0.500	0.150	−0.320	1.990	1.410	−0.450		
Retrieved	0.005	**0.502**	0.142	−0.315	**2.007**	**1.399**	**−0.447**	500	0.000
Retrieved	0.010	**0.515**	0.170	−0.313	**2.084**	**1.293**	**−0.389**	500	0.005
Retrieved	0.050	**0.613**	**0.264**	−0.388	**2.797**	**0.554**	**−0.065**	500	0.031
Initial (ii)		0.100	0.000	0.300	1.000	1.000	0.500		
Retrieved	0.005	**0.491**	**0.210**	**−0.335**	**2.424**	**1.384**	**−0.427**	500	0.001
Retrieved	0.010	0.502	**0.252**	**−0.352**	**2.471**	**1.277**	**−0.367**	500	0.005
Retrieved	0.050	**0.620**	0.234	−0.313	**3.084**	**0.505**	**−0.030**	500	0.029
B)									
True		0.500	0.810	−0.680	2.000	0.550	−0.040		
Initial (i)		0.500	0.810	−0.680	2.000	0.550	−0.040		
Retrieved	0.005	**0.502**	0.812	−0.677	2.011	**0.536**	**−0.031**	500	0.001
Retrieved	0.010	**0.513**	0.810	−0.677	**2.097**	**0.472**	**−0.004**	500	0.005
Retrieved	0.050	**0.595**	0.794	−0.658	**2.807**	**−0.011**	**0.209**	500	0.029
Initial (ii)		0.100	0.000	0.300	1.000	1.000	0.500		
Retrieved	0.005	**0.424**	**0.831**	**−0.743**	**1.975**	**1.284**	**−0.370**	500	0.001
Retrieved	0.010	**0.439**	**0.850**	**−0.747**	**2.064**	**1.160**	**−0.309**	500	0.007
Retrieved	0.050	**0.570**	**0.701**	−0.618	**2.816**	**0.301**	0.033	500	0.033
C)									
True		0.500	0.330	−0.330	1.280	1.040	−0.540		
Initial (i)		0.500	0.330	−0.330	1.280	1.040	−0.540		
Retrieved	0.005	**0.500**	0.330	−0.328	**1.280**	**1.040**	**−0.539**	500	0.001
Retrieved	0.010	**0.500**	**0.331**	**−0.339**	**1.280**	**1.038**	**−0.543**	500	0.003
Retrieved	0.050	**0.520**	0.236	−0.264	**1.310**	**1.010**	**−0.536**	500	0.018
Initial (ii)		0.100	0.000	0.300	1.000	1.000	0.500		
Retrieved	0.005	**0.472**	**0.612**	**−0.523**	**1.167**	**1.053**	**−0.483**	500	0.027
Retrieved	0.010	**0.472**	**0.617**	**−0.540**	**1.168**	**1.046**	**−0.485**	500	0.028
Retrieved	0.050	**0.499**	0.438	**−0.446**	**1.213**	**1.005**	**−0.520**	500	0.033

Values in bold and underlined are those outside the 95% CI of values drawn from a normal distribution.

roughness by rain-splash erosion as much as the other soils. After low and high rainfall intensities, there appeared to be loose erodible material (LEM) on the surface of soil FS. After rainfall and drying, soils FS and CL became brighter whilst soil FSL became slightly darker than the original soil surface. The soils exposed to low intensity rainfall appeared to have developed a rougher surface than those exposed to the high intensity rainfall. After abrasion, all soils became slightly darker than those after the previous treatment. The LEM on the surface of soil FS was removed. Similar LEM was not present on the surface of soils FSL and CL and their surface roughness decreased presumably as a consequence of the abrasion. The material used as an abrader was evidently deposited on the surface of soil FSL (light grey).

3.2. Sensitivity of the model parameter value optimisation

Three sets of data denoted A, B and C were produced to represent variations of the parameters obtained from the soil reflectance. Table 3 shows the 'true' values for these three sets of reflectance data. These parameters were used to generate a total of 23 bi-directional reflectance values for a single value of the solar zenith angle, $i=53°$, zenith viewing angles e that varied between 0° to 50° in increments of 10° and relative azimuth angles ϕ varying from 0° to 180° in increments of 90°. These simulated data were used to closely resemble the illumination and viewing geometry of the soil reflectance measurements.

Pseudo-random noise from a normal distribution was added to reflectance calculations using the three parameter sets A, B and C. A total of 500 data sets of 23 reflectance values each were then inverted using the procedure in Eq. (2). Two cases of initial estimates were used consistently for all data sets to appreciate the importance of the initial estimates on the optimal estimates. The column entitled N in Table 3 shows that in all of the 500 cases the optimisation procedure found a minimum. Following Pinty et al. (1989) the 95% confidence interval was calculated for the known average and randomly generated standard deviation. None of the values were outside that interval which suggests that the one tailed test cannot reject the null hypothesis that there is no significant difference between the average parameter value and that expected from a normal distribution with a known mean. Despite the appearance of considerable variation in the parameter values they are within the range of values expected of a normal distribution with a standard deviation defined by the added noise. The results of initial estimates (i) that were identical to the true value, showed the expected reduction in accuracy as introduced (external) noise increased from 0.05% to 5%. The RMSE of the optimization procedure was smaller than the external noise added to the reflectance data. Initial estimates (ii) that were arbitrarily set to be different from the true values had RMSE that were very similar to those values from experiment (i). These results suggest that the optimisation procedure is not sensitive to the initial estimates. Following Pinty et al. (1989) the 95% CI of each parameter was calculated for each sample of 500 estimates assuming a normal distribution and that the true mean parameter value was known. Average values of the parameters that did not fall within their respective confidence intervals are shown as bold and underlined. The results indicate a tendency for bias in the estimates of the parameter values that is associated with the initial estimate. The origin of this bias in the estimates is not clear however it is likely that the explanation is related to the angular sampling frequency (Pinty et al., 1989). Despite this uncertainty, the available highly resolved spectral

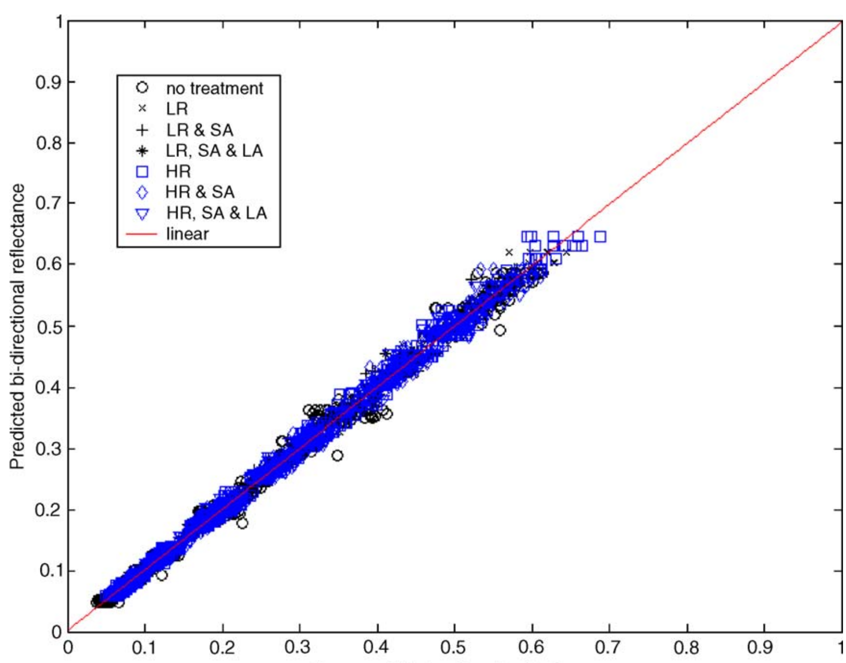

Fig. 3. Comparison between measured and calculated bi-directional reflectance of five wavebands (440 nm, 550 nm, 650 nm, 850 nm and 1650 nm) for several treatments of all soil types. LR – low intensity rainfall; HR – high intensity rainfall; SA – short duration abrasion; and LA – long duration abrasion.

Table 4
Optimised values for the parameters of Jacquemoud et al. (1992) bi-directional soil spectral reflectance model

Sample	Soil type	Rainfall	Abrasion	Bi-directional reflectance model parameters					
				b	c	h	b'	c'	RMSE
10	FS	None	None	0.15	−0.32	1.99	1.41	−0.45	0.022
11	FS	Low	None	0.24	−0.58	1.75	1.39	−0.61	0.020
12	FS	None	Short	−0.29	−0.31	1.97	1.81	−1.01	0.019
13	FS	None	Long	−0.14	−0.40	2.00	1.51	−0.89	0.022
14	FS	High	None	0.19	−0.60	2.00	1.33	−0.53	0.021
15	FS	None	Short	1.48	−1.08	1.99	0.56	0.15	0.022
16	FS	None	Long	1.11	−1.02	2.00	0.19	0.11	0.020
20	FSL	None	None	0.81	−0.68	2.00	0.55	−0.04	0.018
21	FSL	Low	None	1.21	−0.61	1.27	1.05	−0.29	0.016
22	FSL	None	Short	1.18	−0.69	1.58	0.76	−0.24	0.023
23	FSL	None	Long	0.52	−0.41	1.61	1.28	−0.60	0.021
24	FSL	High	None	0.82	−0.73	1.99	0.27	0.04	0.014
25	FSL	None	Short	1.15	−0.86	1.64	0.97	−0.16	0.013
26	FSL	None	Long	1.08	−0.85	1.99	0.04	0.17	0.013
30	CL	None	None	0.33	−0.33	1.28	1.04	−0.54	0.027
34	CL	High	None	−0.10	−0.32	1.69	1.36	−0.70	0.010
35	CL	None	Short	0.12	−0.35	1.59	1.34	−0.56	0.009
36	CL	None	Long	0.23	−0.40	1.53	1.28	−0.53	0.009

information and a high overall accuracy of the estimation procedure (0.012 average of the RMSE) is believed to be sufficient for the accurate retrieval and interpretation of the model parameter values.

3.3. Bi-directional (spectral) soil reflectance model performance

All of the angular measurements of reflectance (440 nm, 550 nm, 650 nm, 850 nm and 1650 nm) of different soils and treatments were inverted against the model using the model parameters defined previously. Fig. 3 shows the results for the observations plotted against the calculations. The relationship between observations and calculations showed a good agreement (RMSE = 0.003) and plotted along the 1 : 1 line. The spectrum of the single scattering albedo was fitted using the same illumination geometries and the remaining model parameters. The model inversion procedure was stratified using soil type and treatment. The optimised values of each model parameter for each soil type and treatment and an assessment of accuracy are shown in Table 4. Fig. 4 shows the results of the observed spectra (450–2450 nm) against the calculated spectra for all soil types but with no treatment. The

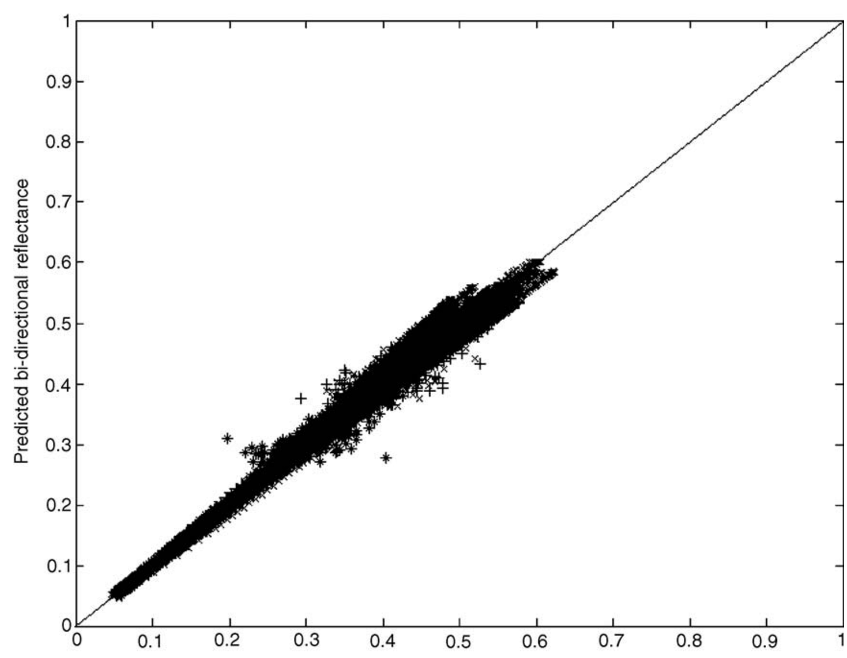

Fig. 4. Comparison between measured and calculated bi-directional spectra (450–2450 nm) of soil FS (×), soil FSL (+) and soil CL (*) for no treatment.

results showed a very good agreement with a slightly reduced level of accuracy (RMSE = 0.02) relative to that of the case with five wavebands but continue to plot along the 1 : 1 line.

Soil CL has values of the roughness parameter h that are much smaller than those of the other soil types (Table 4). This suggests that optically the surface appears much rougher than the other soils and is caused by small shadows behind individual particles and micro-aggregates (Cierniewski, 1987; Hapke, 1963). The value of h increased after high intensity rainfall and then it decreased as abrasion continued. This pattern suggests

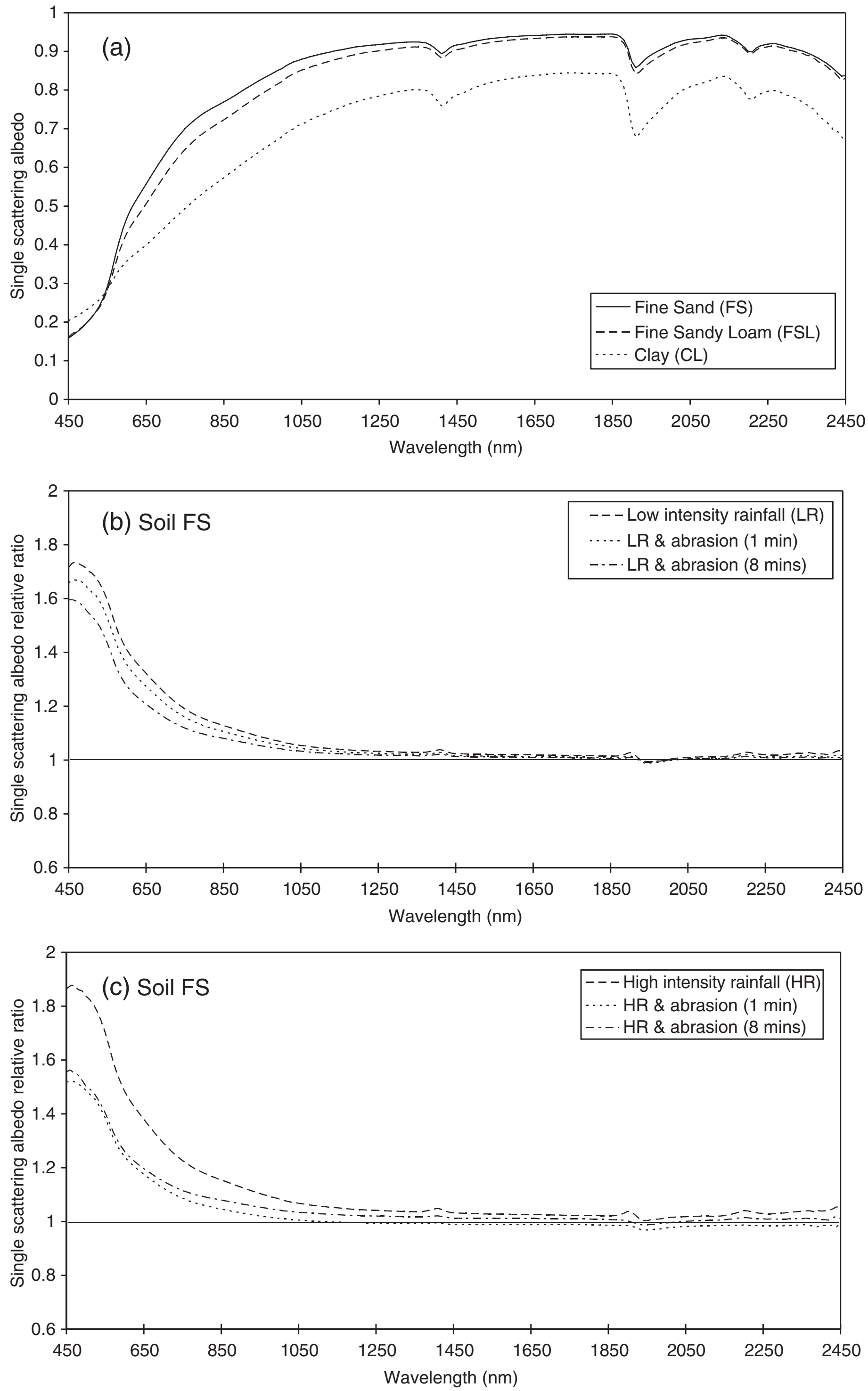

Fig. 5. The single scattering albedo (SSA) estimated using the bi-directional model of soil spectral reflectance for: (a) all replicates of untreated soils, soil type FS divided by its untreated SSA spectra after (b) low intensity rainfall and aeolian abrasion and (c) high intensity rainfall and aeolian abrasion; soil type FSL divided by its untreated SSA spectra after (d) low intensity rainfall and aeolian abrasion and (e) high intensity rainfall and aeolian abrasion; soil type CL divided by its untreated SSA spectra after (f) high intensity and aeolian abrasion.

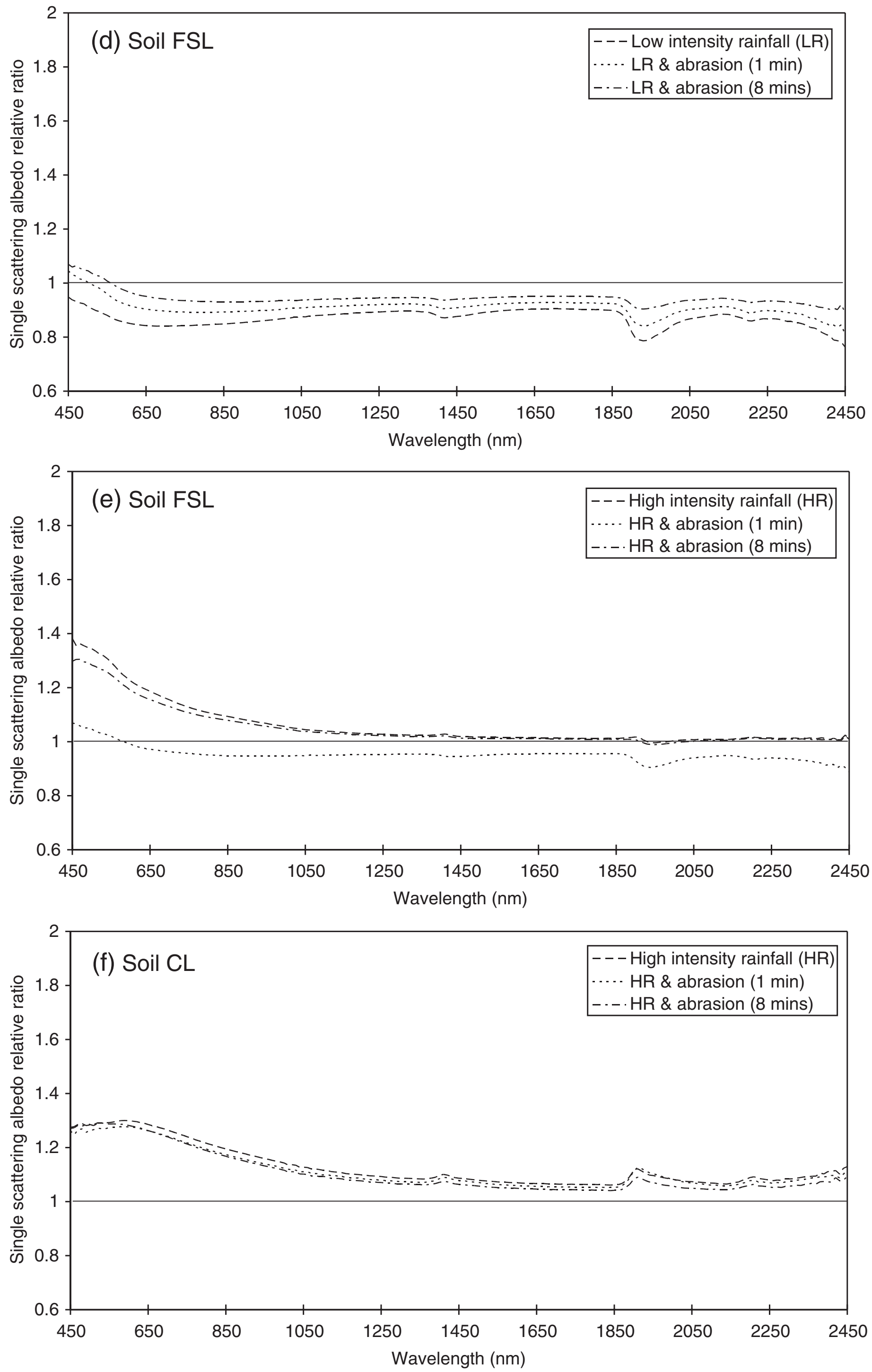

Fig. 5 (*continued*).

that the surface decreased its roughness after rainfall and the abrasion increased the roughness. The large magnitude of the values for the b' and c' parameters suggests that the soil is predominantly forward scattering. After rainfall the forward scattering increased in magnitude, presumably as a consequence of the smooth surface. However, the forward scattering decreased during wind tunnel abrasion as the surface returned to a slightly rougher condition (Table 4).

Soil FSL showed a considerable decrease in the value of h after low intensity rainfall and then an increase after the initial abrasion (Table 4). This pattern indicated that the surface became rough after the low intensity rainfall and then decreased its roughness during the abrasion process. Unlike the other soil types, the untreated soil FSL was dominated by backward scattering of reflectance. After the initial abrasion the reflectance increased in backward scattering and then after the longest duration of abrasion the surface reflectance became forward scattering despite the absence of any change in the roughness parameter h. After high intensity rainfall the value of h for soil FSL was similar to that of the untreated soil. After the initial abrasion, it decreased and then increased after the prolonged abrasion (Table 4). The surface remained backward scattering in its untreated state and after high intensity rainfall. It remained backward scattering after the initial abrasion and after prolonged exposure.

The untreated soil FS had a value for h which was similar to that of the untreated soil FSL indicating a similarly smooth initial surface (Table 4). The value of h for soil FS decreased after low intensity rainfall and then increased to approximately the same level as the untreated surface. This pattern indicated that the rainfall caused the surface to increase in roughness and the abrasion caused it to become as smooth as the untreated surface. The large magnitude of the values for the b' and c' parameters indicated that soil FS is dominated by forward scattering. The forward scattering remained largely unaffected by the low intensity rainfall but the initial abrasion caused an increase in forward scattering. Prolonged exposure to abrasion reduced the forward scattering. It appeared that the initial abrasion after low intensity rainfall did not change the roughness but increased the forward scattering. The same soil FS responded very differently to high intensity rainfall (Table 4). The value of h remained approximately the same as the untreated value indicating that the surface remained similarly smooth. However, the untreated soil, dominated by forward scattering, changed to one of mixed scattering after the high intensity rainfall. Furthermore, despite the absence of any change in roughness the soil surface became backward scattering after initial abrasion. The dominance of this type of scattering increased with prolonged exposure to abrasion.

3.4. Single scattering albedo (SSA) spectra

The single scattering albedo (SSA; ω) spectra for wavelengths between 450 nm and 2450 nm calculated by the model (Eq. (1)) for all three soils prior to any treatment are shown in Fig. 5a. The SSA of soil FS is barely significantly different in most wavelengths from that of soil FSL. Significant difference may be detected using a RMSE = 0.02 (Table 4). In this case, the SSA of soil FSL appears to be significantly smaller than that of soil FS between 500 nm and 1410 nm in the near-infrared (NIR ca. 1000 – 1800 nm) region. The SSA of soil FS and that of soil FSL appears to be larger than the SSA of soil CL in most of the wavelengths. The exceptions are those bands less than 500 nm in the visible (VIS ca. < 1000 nm) region. In this region, soil CL has the largest SSA which may be attributed to iron-oxide phases (goethite and haematite). However, for all other wavelengths the SSA is ~10% smaller than soils FS and FSL. All soils showed evidence of narrow and well-defined absorption features at 1400 nm and at 1900 nm and 2200 nm in the short-wave infrared (SWIR ca. 1800 – 2450 nm) region related to water absorbed by clay minerals in general and smectite minerals in particular (Ben-Dor et al., 1999).

The SSA spectra for each treatment were divided by their respective spectrum for untreated soil (Fig. 5b–f). The ratio minimised common and constant features and therefore enhanced differences in the spectra (Ben-Dor et al., 2003). Overall, there appears to be significant differences in the VIS region between soils and for some treatments. The exceptions appear to be soil CL exposed to high intensity rainfall and abrasion (Fig. 5f) and soil FSL exposed to low intensity rainfall and abrasion (Fig. 5d). In both cases, there was a shift in SSA across all wavebands. Soil CL retained large values in the VIS region. The high intensity rainfall applied to soil CL initiated the increased SSA and the wind tunnel abrasion reduced it over time. Wavebands around 600 nm revealed the greatest difference relative to the untreated spectrum; however, features at 1900 nm and 2200 nm were also evident.

Low intensity rainfall for soil FSL reduced reflectance overall but wavebands at 1930 nm and 2450 nm revealed the greatest negative change relative to the untreated spectrum (Fig. 5d). Abrasion increased the SSA and wavebands around 460 nm revealed the greatest positive change relative to the untreated spectrum. High intensity rainfall affected soil FSL differently and caused changes to the SSA spectra mainly in the VIS region (Fig. 5e). The waveband with the greatest positive change relative to the untreated spectrum was evident around 470 nm. Initial abrasion reduced significantly the reflectance across all wavebands so that it was smaller than the untreated spectrum with the exception of values in the region of 450–590 nm. The wavebands with the greatest negative change relative to the untreated spectrum were evident at 1940 nm and 2440 nm. After abrasion the reflectance in all wavebands increased to approximately the same amount as that after the high intensity rainfall.

The SSA spectra for soil FS also increased after low intensity rainfall but the changes were confined mainly to the VIS region (Fig. 5b). Wind tunnel abrasion reduced over time the SSA spectra in the VIS region. The waveband with the greatest positive change relative to the untreated spectrum was evident around 470 nm. This waveband was also the site of the greatest positive change in the spectrum for soil FS after high intensity rainfall (Fig. 5c). The greatest change in wavebands after this treatment was also found in the VIS region. Initial wind tunnel abrasion reduced slightly the reflectance in all wavebands and decreased that in the NIR and SWIR wavebands to values smaller than the untreated spectrum. After 8 min duration of abrasion, the reflectance had increased in all wavebands but with only small changes in the region between 450 and 590 nm.

Table 5a
Ordinary RDA with forward selection removal of multicollinear variables to explain the variation in reflectance using soil types and soil treatments

	All soils and treatments	
Axes	1	2
Eigenvalues	0.59	0.14
Model parameters–environment correlations	0.89	0.79
Cumulative percentage variance:		
of model parameters data	59.0	73.9
of model parameters–environment relation	78.9	98.3

Table 5b
Explained variance, P-values and F statistics in RDA with forward selection removal of multicollinearity for predicting model parameter values (ranked according to the variance explained during forward selection)

Treatment variables	Explained variance (%)	P-value	F statistics
Marginal effects			
Soil FSL	22	–	–
Soil CL[a]	16	–	–
LR, SA & LA	13	–	–
HR, SA & LA[a]	12	–	–
LR, SA	8	–	–
LR	6	–	–
HR	4	–	–
No treatment (prepared)	3	–	–
Soil FS	3	–	–
HR & SA	0	–	–
Conditional effects			
Soil FSL	22	0.03	4.60
LR, SA & LA	18	0.04	4.49
Soil FS	16	0.01	5.10
No treatment (prepared)	4	0.31	1.29
HR	7	0.14	2.37
LR & SA	3	0.27	1.32
HR & SA	2	0.61	0.55
LR	3	0.34	1.03

Shading indicates those variables that are considered not statistically significant by using a threshold around 15%. LR – low intensity rainfall; HR – high intensity rainfall; SA – short duration abrasion; and LA – long duration abrasion.

3.5. Canonical ordination (redundancy analysis)

The results of the redundancy analysis (RDA) between bi-directional soil spectral reflectance model parameters and soil treatments are shown in Tables 5a and 5b. The eigenvalues in Table 5a measure the importance of each of the canonical axes. Table 5a provides statistics for the first two canonical axes for analysis of all soil types and treatments. The first axis explains 59% of the variation whilst the second axis explains 14%. Thus, 73% of the variation in the data is explained by the first two axes. In addition, the relationship between the model parameter data and the treatments for each axis is very strong. However, in constrained analysis (such as RDA) a large correlation between these components does not mean that an appreciable amount of the model parameter data is explained by the treatment data (Ter Braak, 1988). The amount of variation between the model parameters and the treatments is explained by each axis and is given as a cumulative percentage on the bottom line of Table 5a. Approximately 79% of the variation is explained by the first axis and the second axis provides only an additional 19%.

Fig. 6 provides a visual explanation for these statistics. The elliptical dashed zones provide the approximate extent of the soil types. The model parameters are separated into distinct groups oriented approximately along the axes. Model parameters c and b' are strongly related to the negative direction of axis 1, whilst c' and b are less strongly related to the positive direction of the same axis. The significance of this grouping is that specular and diffuse information is important for axis 1 but that the specular terms and diffuse terms of the model are not separated. Approximately 60% of the variation in the model parameters may be explained by canonical axis 1. In contrast, h is more closely related to the negative direction of the second axis, based on its proximity to that axis, than any other axis direction. Approximately 14% of the variation primarily in the h parameter may be explained by canonical axis 2. It also appears that variation along axis two separates parameters b and

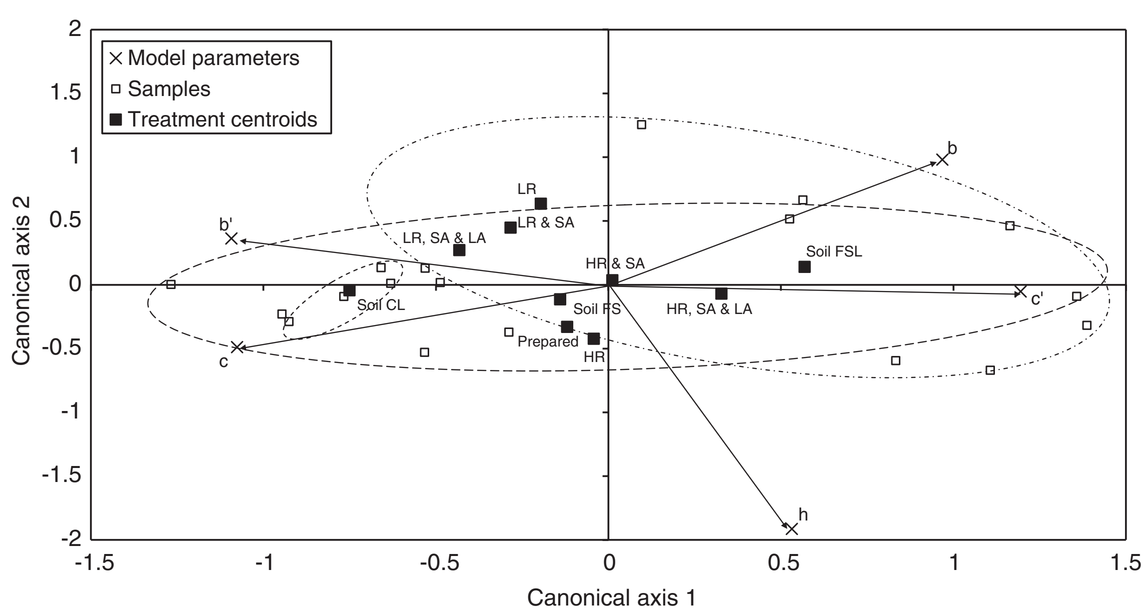

Fig. 6. Ordination diagram of redundancy analysis showing the relationships between model parameters and the ordination axes and the correlations between all soil types and treatments and ordination axes. LR – low intensity rainfall; HR – high intensity rainfall; SA – short duration abrasion; and LA – long duration abrasion. The differently dashed oval shapes indicate the approximate envelope of variation in samples for each soil type and are centred on the soil type centroid (Soil FS, Soil FSL and Soil CL).

b' in the positive direction from the parameters c and c' in the negative direction, i.e., the latter set of parameters are positively related (albeit weakly) to the h roughness parameter.

Table 5b provides a list of variables and their explanation of variance and significance during the forward selection process. The marginal effects are a list of the individual environmental variables in order of the variance they explain singly (Ter Braak, 1988). It can be seen from either the table or Fig. 6 that soil type FSL and treatment involving high intensity rainfall and short and long duration of abrasion (HR, SA and LA) are highly positively correlated with canonical axis 1. Soil type CL and treatment involving low intensity rainfall and short and long duration of abrasion (LR, SA and LA) are negatively correlated with canonical axis 1. However, initial high intensity rainfall (HR) is strongly correlated with axis 2 in the negative direction and approximately aligned with the h parameter. The centroid for low intensity rainfall alone (LR) and that combined with short duration abrasion (LR and SA) are correlated with axis 2 in the positive direction and negatively correlated with the h parameter. Notably, high intensity rainfall and short abrasion treatments (HR and SA) are not associated with any of the variability in model parameter values.

The lowest parts of Tables 5a and 5b shows the conditional effects (Ter Braak, 1988) of the redundancy analysis and provides the environmental variables in order of their inclusion in the model, together with the additional variance each variable explains at the time it was included and the significance of the variable at that time (P-value). The results reveal that the only statistically significant (5% level) variables for explaining variation in the model parameter values are soil types FSL and FS and the treatment involving low intensity rainfall and short and long duration abrasion. Furthermore, soil CL and the treatment using high intensity rainfall and short and long duration abrasion were redundant variables and could be explained completely by other combinations of variables.

4. Discussion

The diversity of reflectance among a wide variety of soil samples has been explained by Stoner and Baumgardner (1981) with five basic curves. Similar results have been found by Price (1990) and Huete and Escadafal (1991). However, we know intuitively that variation of the surface characteristics will cause considerable variation in the spectral reflectance within a soil type. Chappell et al. (2005) demonstrated that there was as much variation in the on-nadir reflectance of soil surfaces generated within soil types as that found between soil types. That work was limited to the spectral composition of the soil surface changes. The results of the ordination analysis presented here used the spectral reflectance model parameter values to summarise the scattering characteristics including an estimation of roughness. The results are consistent with Chappell et al. (2005) because they show that the variation in the model parameter values is explained by a combination of the soil types and the treatments. Notably, changes in the surface of soil CL and variability due to high intensity rainfall could be completely explained by linear combinations of the other soil types and treatments. However, variability (ca. 18%) in the soil spectral reflectance model parameter values was also explained by low intensity rainfall combined with short and long duration abrasion (Table 5b). It appears that variation explained by high intensity rainfall was redundant because it created a crust similar to that produced by low intensity rainfall but which was thicker and could not be easily abraded. Zobeck (1991a) compared the abrasion of crusts created by low and high intensity rainfall and found abrasion resistance to increase rainfall intensity. Therefore, for a given duration of abrasion there was little variation in the behaviour of the soil surface. Evidently, the duration of abrasion would, in future experiments, need to be much longer to ensure that variability in this treatment was not redundant.

Perhaps more importantly, the results of the redundancy analysis (Fig. 6) show that axis 1 is dominated by the nature of the scattering from the soil surfaces with different treatments. There is not a simple separation according to the forward and backward scattering of reflectance. All soils show evidence of backward and forward scatterings that depend on their treatment. This finding is consistent with the observations of the variation in model parameter values (Table 4). Furthermore, the variability in roughness as indicated by the h parameter is also related (albeit not very strongly) to the type of scattering. In general, it appears from Fig. 6 that low intensity rainfall (and short duration abrasion) was associated with a decrease in the h parameter and therefore with an increase in roughness. In contrast, high intensity rainfall was associated with an increase in the h parameter and therefore with a decrease in roughness. Notably, high intensity rainfall and short duration abrasion was not related to any of the model parameters shown in Fig. 6. This was evidently because of the inability of the short duration abrasion to change the soil surface characteristics. As described in the previous paragraph, the high intensity rainfall combined with long duration abrasion made little impact on the roughness but was strongly correlated with the c' parameter. In contrast, low intensity rainfall combined with long duration abrasion was strongly correlated with the b' parameter. These results suggest that the rainfall combined with abrasion is associated with forward scattering and that the specific relationship with the model parameters is related to the intensity of rainfall. More fundamentally, rain-splash is related to the development of a soil crust (McIntyre, 1958). The surface of a crust usually comprises smaller (clay) particles than those within or beneath the crust usually as a consequence of the preferential movement of particles near the surface resulting in an upper skin seal (crust) and deeper wash-in region (Ben-Dor et al., 2003). Soil micro-aggregates may also be broken during rainfall. Thus, the orientation of the particles and their distribution over the surface is altered due to rainfall. The extent of crust development and aggregate stability is highly dependent on soil type which itself depends on the organic matter and sand, silt and clay fractions. Furthermore, abrasion of the soil surface by the impact of saltating particles is well known to erode material and may either increase or decrease the surface roughness depending on its status, e.g., loose erodible material on a crusted surface. A detailed analysis for each soil and its response to treatments is described below.

4.1. Erodibility of soil CL

The forward scattering of the untreated soil was related to the relatively homogeneous optical properties (Hapke, 1963) of soil CL. The increase in (the roughness parameter) h after the rainfall and the increase in forward scattering demonstrated that the surface became smoother and the particles at the surface became more similar than the untreated (prepared) surface. In addition, the SSA of soil CL increased and wavebands around 600 nm, 1900 nm and 2200 nm also changed after high intensity rainfall which is consistent with a decrease in clay (probably haematite or goethite) sized material at the surface (Ben-Dor et al., 1999). Thus, there is direct evidence for smoothing and sealing of the surface with small clay-sized material as a consequence of rain-splash. During abrasion the SSA decreased, the roughness parameter h decreased and the forward scattering of reflectance decreased. These characteristics are in opposition to those for the development of a surface seal and suggest strongly that the abrasion process selectively removed material from the surface seal.

4.2. Erodibility of soil FSL

The untreated soil FSL was dominated by mixed or isotropic scattering and appeared very smooth relative to soil CL, despite its relatively coarse particle size (Table 2). Mixed scattering of reflectance is expected from a mixture of particles including opaque spheroids with smooth surfaces, irregular translucent particles and particles with smooth surfaces that reflect light specularly (Hapke, 1963). After low intensity rainfall, the roughness parameter decreased, the SSA decreased and the reflectance became backward scattering. Backscattering is caused by particles at the surface that are larger than a wavelength and hide shadows and is expected from opaque surfaces with fairly rough faces orientated at random (Hapke, 1963). A reduction in the reflectance at waveband 1930 nm and a decrease in that of the VIS region suggested that the clay fraction at the surface decreased. These characteristics suggest that in this soil rain-splash washed in the small clay-sized material coated with iron oxides, leaving at the surface larger particles/aggregates with few iron oxides. After initial abrasion, the reflectance became more backward scattering, the SSA increased and the roughness parameter increased. This pattern is consistent with the preferential removal of material at the surface by the abrasion process exposing the washed-in clay material. However, the development of backscattering reflectance is likely to be a consequence of the poorly sorted nature of the exposed material. The reflectance of the soil surface became forward scattering after 8 min of abrasion and the SSA increased to a level similar to that of the untreated soil despite the absence of any change in the roughness parameter. It appears that the prolonged abrasion has progressively eroded into the washed-in layer and exposed at the surface a coarse homogeneous material with scattering properties similar to soil CL.

Between its untreated state and that after high intensity rainfall, there appeared to be little change in the roughness parameter and the backward scattering of reflectance of soil FSL. However, the treatment caused an increase in SSA mainly in the VIS region, which suggested that despite the absence of a change in the roughness parameter there was an increase in the number of large aggregates with iron oxide coatings at the surface as part of the seal development during the rain-splash process. The high intensity rainfall smoothed the soil surface and created a crust. After initial abrasion, the roughness parameter decreased (roughness increased), the soil surface remained backward scattering of reflectance and decreased its SSA. In particular, a large reduction relative to the untreated surface in wavebands 1940 nm and 2440 nm signaled a reduction in clay-sized material at the surface and an increase in aggregate size. It appeared that the initial abrasion removed those small aggregates brought to the surface during the rain-splash and exposed a mixture of particles with fewer clay coatings. After prolonged abrasion, the surface reflectance was strongly backward scattering and the roughness parameter increased to a level similar to that found after the high intensity rainfall. The single SSA spectrum was considerably larger, mainly in the VIS region, than that of the untreated surface and similar to that spectrum found after rainfall. It appears that the prolonged abrasion preferentially removed large dark-coloured particles.

4.3. Erodibility of soil FS

Low intensity rainfall on this soil produced a similar response to that of soil FSL after high intensity rainfall. The roughness parameter decreased after low intensity rainfall, forward scattering remained largely unaffected from that of the untreated surface and the SSA increased particularly in the VIS region. These results suggest that the untreated surface was relatively smooth and that the rainfall increased the roughness by bringing particles/aggregates or loose erodible material (LEM) to the surface with clay coatings which changed the colour and increased the reflectance in the VIS region. Abrasion over time increased the roughness parameter (decreased roughness) by removing those particles/aggregates with clay coatings. Notably, the forward scattering of reflectance was reduced suggesting that the surface was preferentially eroded by the abrasion process and that a more mixed surface was revealed (Chappell et al., 2005).

Soil FS remained as smooth after high intensity rainfall as the untreated surface, the forward scattering of reflectance remained, but the SSA increased again mainly in the VIS region. These results suggested that the high intensity rainfall replaced aggregates at the untreated surface with those that had a greater reflectance and that this translocation during rain-splash did not affect the roughness parameter or the optical scattering of the surface. Initial abrasion did not change the roughness parameter either but it reduced the SSA in the VIS region and shifted the surface to backward scattering of the reflectance. The interpretation of these results is that the removal of the brighter clay material exposed a darker surface in which the number of shadows remained the same but that the size of the particles increased and caused the backward scattering of reflectance.

Prolonged abrasion hardly affected the roughness parameter and the scattering of reflectance but the SSA increased, mainly in the VIS region suggesting a tendency for the preferential selection of particles/aggregates with iron-oxide coatings typical of those readily eroded sand-sized particles of this soil type.

5. Conclusion

Three soils known to be susceptible to wind erosion were modified using rainfall simulation and wind tunnel abrasion experiments. Observations of the changes at the soil surfaces were made and recorded using digital images. Multi-angular spectral measurements of reflectance were also made and inverted against a bi-directional soil spectral reflectance model (Jacquemoud et al., 1992). A comparison of the measurements and calculations for five wavebands showed good agreement with small errors in the accuracy. Furthermore, measurements and calculations of the spectral reflectance between 450 and 2450 nm also showed good agreement and small acceptable variation in accuracy. The model inversion procedure was shown to be relatively insensitive to the starting conditions. Optimised values of the model parameters produced the single scattering albedo (SSA) and a description of the scattering behaviour of the soil surfaces that included an estimate of roughness. The model parameters removed the effect of the measurement conditions (illumination and viewing geometry) on the spectral reflectance.

In common with earlier work (Chappell et al., 2005), the composition of the soil surface changes was inferred from differences between the spectra before and after treatments. The nature of the reflectance scattering and a quantitative estimate of roughness provided additional information about the structural nature of the soil surface changes. The changes detected at the soil surface included amongst others, the presence of a crust produced by rain-splash, the production of loose erodible material covering a rain crust and the selective erosion of the soil surface. Redundancy analysis showed that much of the variation in the values of the soil reflectance model parameters was explained by the scattering properties and the roughness parameter of the soil surfaces. However, there was no simple separation of the soils and treatments between backward and forward scattering of reflectance. In common with earlier work (Chappell et al., 2005), variation in the soil surface reflectance was not explained solely by soil type. Instead, low intensity rainfall combined with short and long duration abrasion explained a significant portion of the variation. These findings provide a source of considerable variation in experimental and operational spectral reflectance measurements that has perhaps hitherto been largely ignored. Laboratory soil experiments designed to develop models for natural environment predictions may be biased by their exclusion of variation in natural surface conditions for each soil type. It appears unreasonable to assume that variation of the surface characteristics will not cause considerable variation in the spectral reflectance within a soil type. It is likely that variation in environmental treatments within a soil type is a simple and underestimated source of variation in the characterisation of soil surface erodibility and in the remote sensing of soil. The results demonstrated that readily available information on the composition and structure of the soil surface could be retrieved without interference with the soil or natural processes.

Acknowledgements

This work was funded by an award to AC from the UK Natural Environmental Research Council (NER/M/S/2001/00124). The authors are grateful to the United States Department of Agriculture, Agricultural Research Service for making available the spectroradiometer and the rainfall simulator used in these experiments and to Texas Tech University for generously providing access to the wind tunnel. We are also grateful to Dean Holder for constructing the goniometer and for technical assistance with the operation of the wind tunnel. Assistance from Stefan Jacquemoud with the bi-directional soil spectral reflectance model is also gratefully acknowledged. We appreciated the comments and provocative questions of the anonymous reviewers which did much to improve the manuscript. Any omissions or inaccuracies that remain in the paper are the sole responsibility of the authors.

References

Baumgardner, M. F., Silva, L. F., Biehl, L. L., & Stoner, E. R. (1985). Reflectance properties of soils. *Advances in Agronomy*, *38*, 1−44.

Beale, B., & Fray, P. (1990). *The vanishing continent.* Sydney: Hodder and Stoughton.

Ben-Dor, E., Goldshleger, N., Benyamini, Y., Agassi, M., & Blumberg, D. G. (2003). The spectral reflectance properties of soil structural crusts in the 1.2 to 2.5 μm spectral region. *Soil Science Society American Proceedings*, *67*, 289−299.

Ben-Dor, E., Irons, J. R., & Epema, G. (1999). Soil reflectance. In A. N. Renzc (Ed.), *Remote sensing for the earth sciences*, *Vol. 3 (pp. 111–1888). New York: Wiley.*

Böhner, J., Schäfer, W., Conrad, O., Gross, J., & Ringeler, A. (2003). The WEELS model: Methods, results and limitations. *Catena*, *52*(4), 289−308.

Chappell, A., Zobeck, T., & Brunner, G. (2005). Induced soil surface change detected using on-nadir spectral reflectance to characterise soil erodibility. *Earth Surface Processes and Landforms*, *30*(4), 489−511.

Cierniewski, J. (1987). A model for soil surface roughness influence on the spectral response of bare soils in the visible and near-infrared range. *Remote Sensing of Environment*, *23*, 97−115.

Fryrear, D. W., Saleh, A., Bilbro, J. D., Schomberg, H. M., Stout, J. E., & Zobeck, T. M. (1998). *Revised Wind Erosion Equation (RWEQ). Wind Erosion and Water Conservation Research Unit, USDA-ARS, Southern Plains Area Cropping Systems Research Laboratory. Technical Bulletin No. 1*. http://www.csrl.ars.usda.gov/wewc/rweq.htm

Geeves, G. W., Leys, J. F., & McTainsh, G. H. (2000). Soil erodibility. In P. E. Charman & B. Murphy (Eds.), *Soils their properties and management* (pp. 205−220). New York: Oxford University Press.

Hagen, L. J., Zobeck, T. M., Skidmore, E. L., & Elminyawi, I. (1995). *WEPS technical documentation: Soil submodel. SWCS WEPP/WEPS Symposium. Ankeny, IA*.

Hapke, B. W. (1963). A theoretical photometric function for the lunar surface. *Journal of Geophysical Research*, *68*, 4571−4586.

Hapke, B. W. (1981). Bidirectional reflectance spectroscopy: 1. Theory. *Journal of Geophysical Research*, *86*, 3039−3054.

Huete, A. R., & Escadafal, R. (1991). Assessment of biophysical soil properties through spectral decomposition techniques. *Remote Sensing of Environment*, *35*, 149−159.

Jacquemoud, S., Bater, F., & Hanocq, J. F. (1992). Modeling spectral and bidirectional soil reflectance. *Remote Sensing of Environment*, *41*, 123−132.

Latz, K. R. A., Weismiller, G. E., Van Scoyoc, G. E., & Baumgardner, M. F. (1984). Characteristic variations in spectral reflectance of selected eroded Alfisols. *Soil Science Society American Journal*, *48*, 1130−1134.

Marticorena, B., & Bergametti, G. (1995). Modeling the atmospheric dust cycle: 1. Design of a soil-derived dust emission scheme. *Journal of Geophysical Research*, *100*(D8), 16,415−16,430.

Matlab. (2000). *Users guide: Optimisation toolbox*. Version 2.1 (Release 12). Mathworks Inc.

McIntyre, D. S. (1958). Soil splash and the formation of surface crusts by raindrop impact. *Soil Science*, *85*, 261−266.

McTainsh, G. H., Lynch, A. W., & Tews, K. (1998). Climatic controls upon dust storm occurrence in eastern Australia. *Journal of Arid Environments*, *39*, 457−466.

Pinty, B., & Verstraete, M. M. (1991). Extracting information on surface properties from bidirectional reflectance measurements. *Journal of Geophysical Research*, *96*, 2865−2874.

Pinty, B., Verstraete, M. M., & Dickinson, R. E. (1989). A physical model for predicting bidirectional reflectances over bare soil. *Remote Sensing of Environment*, *27*, 273−288.

Potter, K. N., Zobeck, T. M., & Hagen, L. J. (1990). A micro-relief index to estimate soil erodibility by wind. *Transactions of the American Society of Agricultural Engineers*, *33*(1), 151−155.

Price, J. (1990). On the information content of soil reflectance spectra. *Remote Sensing of Environment*, *33*, 113−121.

Seubert, C. E., Baumgardner, M. F., & Weismiller, R. A. (1979). Mapping and estimating aerial extent of severely eroded soils of selected sites in Northern Indiana. *Institute of Electrical and Electronic Engineers*, 234−239.

Shao, Y., & Leslie, L. M. (1997). Wind erosion prediction over the Australian continent. *Journal of Geophysical Research*, *102*(D25), 30091−30105.

Shao, Y., Raupach, M. R., & Leys, J. F. (1996). A model for prediction of aeolian sand drift and dust entrainment on scales from paddock to region. *Australian Journal of Soil Research*, *34*, 309−342.

Sokolik, I. N., & Toon, O. B. (1996). Direct radiative forcing by anthropogenic airborne mineral aerosols. *Nature*, *381*, 681−683.

Stoner, E. R., & Baumgardner, M. F. (1981). Characteristic variations in reflectance of surface soils. *Soil Science Society American Journal*, *45*, 1161−1165.

Ter Braak, C.J.F. (1988). CANOCO: A FORTRAN Program for Canonical Community Ordination by [partial] [detrended] [canonical] Correspondence Analysis and Redundancy Analysis (version 2.1). Agricultural Mathematics Group, Wageningen, The Netherlands.

U.S. Department of Agriculture. (1989). *The second RCA appraisal: Soil, water, and related resources on nonfederal land in the United States.* Washington, D.C.: U.S. Government Printing Office.

Wagner, L.E. (1995), An overview of the wind erosion prediction system. USDA-ARS/Kansas Ag. Exp. Station, No. 96–205–A.

Zender, C. S., Bian, H., & Newman, D. (2003). Mineral Dust Entrainment And Deposition (DEAD) model: Description and 1990s dust climatology. *Journal of Geophysical Research*, *108*(D14), 4416. doi:10.1029/2002JD002775.

Zobeck, T. M. (1991). Abrasion of crusted soils: Influence of abrader flux and soil properties. *Soil Science Society American Proceedings*, *55*, 1091−1097.

Zobeck, T. M. (1991). Soil properties affecting wind erosion. *Journal of Soil and Water Conservation*, *46*(2), 112−118.